

Structural Strength Analysis of Flight Control Actuator Support System Part Bell Crank LH-Wing Using Finite Element Method on NXXX Aircraft

^{1*}Shofwan Bahar, ²Eflita Yohana, ³Sri Nugroho, ⁴Margiyanto

^{1,2,3,4}Department of Mechanical Engineering, Diponegoro University, Semarang, Indonesia

*Corresponding Author's E-mail: shofwanbahar23@gmail.com

Abstract - Flight control systems are crucial in managing the trajectory of commercial aircraft, ensuring stable and safe flight. This system consists of various components including sensors, controllers, actuators, and communication channels, designed with the constraints of the flight environment in mind. Flight control components are made of lightweight yet durable materials, making them reliable in various flight conditions to withstand shocks, vibrations, and stresses during operation. One of the components in flight control is the bracket and bell crank. By applying the Finite Element Method using MSC Patran and MSC Nastran, an analysis was conducted to understand the data processing process to obtain results in the form of deformations, stresses, and forces acting on the Flight Control Actuator System components. The results of this study indicate that the forces generated during the operation of the pulley to move the aileron can cause loads and stress on the Flight Control Actuator System structure. This has the potential to affect the reliability and performance of the flight control actuator system, which is crucial in maintaining stability, responsiveness, and control of the aircraft during flight.

Keywords: Flight Control System, Bracket, Bell crank, Finite Element Method, MSC Patran and Nastran.

I. INTRODUCTION

Airplanes represent a remarkable technological advancement for the world. Since humans discovered how to fly, global technological progress has accelerated. This is due to the existence of airplanes, which have made communication between countries easier. Airplanes are the most effective and efficient means of transportation. This is because they can cover very long distances in a relatively short time. Furthermore, airplanes can carry large numbers of passengers and cargo in a single flight [1]. Airplane components are critical and require high performance to maintain the safety of the aircraft and other air transportation vehicles, one of which is the actuator system on the aircraft's wings.

Flight Control Systems are crucial for managing the trajectory of commercial aircraft, ensuring stable and safe flight. These systems consist of various components, including sensors, controllers, actuators, and communication channels. These components work together to monitor and adjust control surfaces such as ailerons, elevators, and rudders in real time. The development of FCS has evolved from mechanical controls to electronic and digital technology. In the early stages, mechanical systems were controlled using physical connections. However, the advent of electronic flight control systems marked a significant shift towards the integration of electronic sensors and computers, resulting in significant improvements in accuracy and reliability [2].

The bell crank is a component of the NXXX aircraft's flight control system. It is a crucial component of the NXXX aircraft's flight control system, playing a role in transmitting forces and motions from the actuators to the control surfaces. Its functions encompass various aspects, from changing the direction of the forces applied by the control system to ensuring precise and responsive aileron, elevator, and rudder movements. With its robust and reliable design, the bell crank helps maintain aircraft stability and control during flight. Bellcranks are often used in control mechanisms to change direction or increase the torque of forces according to the aircraft's aerodynamic design requirements. A bell crank is a type of crank lever that changes the direction of motion through an angle, which can vary from 0 to 360 degrees. Among these variations, bell cranks with 90-degree and 180-degree angles are the most used [3].

Analysis of the flight control system actuator is necessary to ensure the structural strength of each component due to the internal forces generated by the actuator, linkage, and other drive mechanisms. Given the complex shape and configuration of the actuator structure in the flight control system, this analysis can be performed using finite element analysis (FEA). The finite element method is a numerical technique used to perform finite element analysis of any physical phenomenon [4]. This method allows the identification of stress distribution, deformation, and critical

areas that have the potential for failure. In this case, MSC Patran is used for geometry modeling and meshing, while MSC Nastran is used to analyze the structural response to aerodynamic loads, actuator forces, and other operational conditions.

II. MATERIAL AND METHOD

2.1 Upper Bracket

The upper bracket (Fig. 1) on the Flight Control Actuator Support System is a structural component that serves as the primary mounting for the flight control actuator. Made of 7050 aluminum, this bracket is designed to withstand dynamic loads and ensure actuator stability.

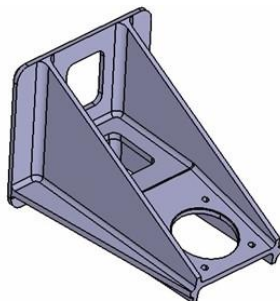


Figure 1: Upper bracket [5]

2.2 Lower Bracket

The Lower Bracket (Fig. 2) on the Flight Control Actuator Support System is a structural component that supports the lower part of the flight control actuator. This bracket transfers the load from the actuator to the aircraft structure, ensuring the stability and precision of flight control movements.

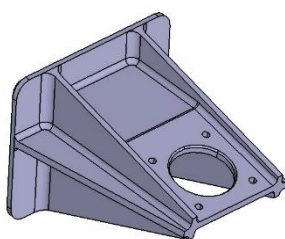


Figure 2: Lower bracket [5]

2.3 Bell crank

The bell crank (Fig. 3) in a Flight Control Actuator Support System is a hinged lever-shaped mechanical component that changes the direction of force or movement in the flight control system. This component is used to transmit and divert force from the actuator to the cables or rods that control surfaces such as the ailerons, elevators, and rudder.

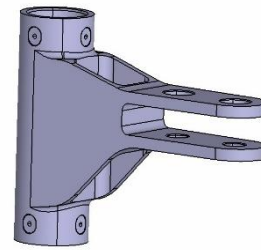


Figure 3: Bell crank [5]

2.4 Material Stiffness

Material stiffness is the ability of a material to resist deformation or change in shape when a load is applied. This is measured by the modulus of elasticity (E) (Eq. 1), which indicates the extent to which a material will deform within its elastic limits. The higher the stiffness value, the smaller the deformation that occurs under load. Material stiffness affects structural behavior in responding to forces and stresses.

$$E = \frac{\sigma}{\epsilon} \quad (1)$$

Where E = modulus of elasticity (Pa or N/m²); σ = stress (Pa or N/m²); ϵ = strain.

2.5 Moment of Inertia

Inertia is the tendency of an object to maintain its state of motion, whether at rest or moving in a straight line at a constant speed, unless an external force changes it. Moment of inertia is a measure of an object's resistance to rotation about its axis. Mathematically, the moment of inertia is expressed as the product of the particle's mass and the square of its distance from the axis of rotation. The magnitude of an object's moment of inertia can be obtained from its linear velocity when viewed from its rotational kinetic energy [6]. The moment of inertia value can be obtained using the following equation 2:

$$I = \frac{\pi}{4} (R_1^4 - R_2^4) \quad (2)$$

Where I = moment of inertia (m⁴); R_1 = outer radius of the cylinder (m); R_2 = inner radius of the cylinder (m).

2.6 Deformation

Deformation is a change in shape due to stress on metal caused by the expansion of weld metal during the heating and cooling process, which has the potential to reduce the strength of the ship's structure as well as the ship's operational efficiency. The deformation that occurs can be in the form of elastic deformation or plastic deformation. Elastic deformation occurs if the load acting on the material is removed and then the material can return to its original shape. Conversely,

plastic deformation occurs if the load acting on the material is removed, but the material cannot return to its original shape [7]. The deformation value can be obtained using the following equation 3:

$$\delta = \frac{FL}{AE} \quad (3)$$

Where δ = change in length (m); F = tensile or compressive force (N); L = initial length of the object (m); A = cross-sectional area of the object (m²); E = modulus of elasticity (Pa or N/m²).

2.7 Margin of Safety

Margin of safety is an engineering concept that refers to the amount of additional capacity built into a system. This additional capacity allows the system to function safely even when subjected to conditions that exceed the load it was designed to handle (known as the design load) [8]. To ensure an object does not experience failure before reaching maximum stress, the MS value of the object's structure must be positive. The margin of safety value can be obtained using the following equation 4:

$$MS = \frac{\sigma_{allowable}}{\sigma_{applied}} - 1 \quad \text{or} \quad = \frac{Load_{allowable}}{Load_{applied}} - 1 \quad (3)$$

Where MS = Margin of Safety; $\sigma_{allowable}$ = maximum allowable stress value; $\sigma_{applied}$ = value of stress applied to the structure; $Load_{allowable}$ = maximum allowable force value.

2.8 Finite Element Analysis

Finite Element Analysis (FEA), also known as the finite element method, is a method that has proven to be quite successful in analysing stresses occurring in a structure. The basic concept of this method is discretization, which is dividing an object into smaller shapes that still possess the same properties as the original material. This method is widely used to solve engineering problems and mathematical problems of physical phenomena. The types of technical and physical-mathematical problems that can be solved with the finite element method are divided into two groups: the structural analysis group and the non-structural problem group [9].

This method can solve complex structural problems in solid mechanics to produce solutions in the form of stress, strain, deflection, and even fatigue life. The advantages of the FEA method include the efficient use of time and cost at a minimum, this method can even be used before the actual prototype using MSC Patran and Nastran software.

2.9 AL-7050-T7451-AMS_4050

The 7050-T7451 aluminium alloy is known for its high strength and good corrosion resistance, often used in the aviation and automotive industries. With a primary composition of aluminium, zinc, and magnesium, this alloy has a microstructure consisting of recrystallized grains, non-recrystallized sub-grains, and primary precipitates that strengthen the metal matrix. The heat treatment process of T7451 improves the mechanical properties, making it ideal for structural applications such as aircraft wings and components that require resistance to high loads and fatigue. The microstructure of the 7050-T7451 aluminium alloy consists of various regions, namely: recrystallized grains, non-recrystallized sub-grain structures, various types of primary precipitates [10].

Table 1: Mechanical Properties Al 7050-T7451

Specification	AMS 4050															
	Plate															
	T7451															
Temp	0.250-1.500		1.501-2.000		2.001-3.000		3.001-4.000		4.001-5.000		5.001-6.000		6.001-7.000		7.001-8.000	
Thickness, in	A	B	A	B	A	B	A	B	A	B	A	B	A	B	A	B
Mechanical Properties																
F_u , ksi	74*	76	74	76	73*	75	72	74	71*	73	70*	72	69	72	68	71
L	74	76	74*	76	73*	75	72	75	71*	74	70	73	69	72	68	71
LT	74	76	74*	76	73*	75	72	75	71*	74	70	73	69	72	68	71
ST	68	72	68*	71	67	70	66	69	66	68	65	67
F_u , ksi
L	64*	67	64*	66	63*	66	62*	65	61*	65	60	63	59	62	58*	63
LT	64	66	64	66	63*	66	62	65	61	64	60	62	59	62	58	61
LT	64	66	64	66	63*	66	62	65	61	64	60	62	59	62	58	61
ST	59	61	57	60	57*	60	57	59	56	58	55*	58
F_u , ksi
L	63	64	62	64	61	64	60	63	58	61	57	59	56	59	55	57
LT	66	68	67	69	66	69	65	68	64	67	63	66	60	63	59	62
LT	66	68	67	69	66	69	65	68	64	67	63	66	60	63	59	62
ST	63	66	63	66	63	66	62	64	60	63	59	62
F_u , ksi
L	43	44	44	45	43	45	44	45	43	45	43	45	44	46	44	46
LT	43	44	44	45	43	45	44	45	43	45	43	45	44	46	44	46
LT	43	44	44	45	43	45	44	45	43	45	43	45	44	46	44	46
ST
F_u , ksi
(eD = 1.5)
L	107	110	109	112	108	111	107	111	107	111	105	110	107	112	103	108
LT	109	112	111	114	110	113	109	113	108	113	107	112	109	114	107	112
ST
(eD = 2.0)
L	140	145	142	146	141	144	140	144	138	144	137	142	136	143	132	138
LT	140	144	142	146	141	145	141	145	139	145	138	144	139	146	137	143
ST
F_u , ksi
(eD = 1.5)
L	86	89	89	92	89	93	90	94	90	95	91	94	84	89	83	87
LT	87	89	90	92	89	94	90	95	90	95	91	94	85	90	84	88
ST
(eD = 2.0)
L	101	104	104	107	104	109	104	109	105	110	105	108	99	105	98	102
LT	103	106	106	110	106	111	106	111	106	111	106	110	99	105	98	103
ST

2.10 Software MSC PATRAN/NASTRAN

PATRAN is a Finite Element Analysis (FEA) pre- and post-processing software that provides various tools ranging from solid modeling, meshing, analysis setup, and so on. Meanwhile, NASTRAN MSC Nastran is the most widely used Finite Element Analysis (FEA) solver in the world. When it comes to simulating stress, dynamics, or vibration of complex systems in the real world, MSC Nastran remains the best and most trusted software in the world – period. Today, manufacturers of everything from spare parts to complex assemblies choose FEA solvers that are reliable and accurate enough to be certified by the FAA and other regulatory bodies [11]. Each software is developed by Hexagon, a software technology development company based in Sweden.

2.11 Problem Solving Flowchart

In the analysis, a flowchart was created to illustrate the problem-solving process. The flowchart of the research conducted by the author is shown in Diagram Fig. 4 below.

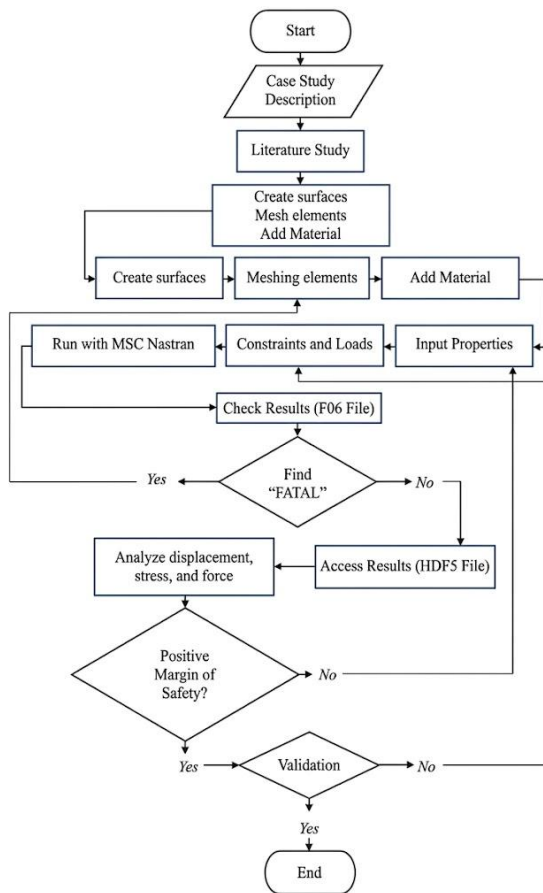


Figure 4: Problem Solving Flowchart

III. RESULTS AND DISCUSSIONS

3.1 Schematic Diagram of Flight Control Actuator

A Schematic diagram is a diagram that shows the direction and magnitude of the relative forces acting on a given object. Free-body diagrams with different loading variables will produce different values. Figure 5 shows the forces generated by the pull of the lever and the pressure exerted by the aileron cable.

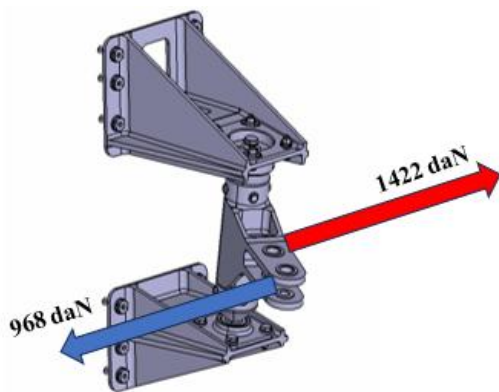


Figure 5: Schematic Diagram of Flight Control Actuator

Based on the free body diagram of the force direction of the aileron cable regulating the bell crank above, the following equation 4 can be formed.

$$\Sigma F = P1 \text{ aileron cable} - P2 \text{ aileron cable} \quad (4)$$

$$\Sigma F = 1422 - 968$$

$$\Sigma F = 454 \text{ daN}$$

3.2 Bearing Strength Plane

Bearing strength plane is a calculation to assess strength based on the compressive force applied by the fastener around the contact area between the fastener and the material. Bearing strength refers to the material's ability to withstand loads applied directly to the contact area without experiencing damage such as cracking or significant deformation. In structural design, it is important to ensure that the load applied to a rivet or other structural element does not exceed the bearing capacity or strength of the material used. If the load exceeds the bearing capacity, cracking or other structural damage can occur.

The equation 5 for calculating the Margin of Safety is as follows:

$$MS = \frac{\sigma_{\text{allowable}}}{\sigma_{\text{applied}}} - 1 \Rightarrow \frac{Ftu \times 0.689}{\frac{\text{Force}}{D \times \text{Thickness}}} - 1 \quad (5)$$

3.2.1 Bell Crank Group

The following are the results of the bearing strength plane calculations for the bell crankgroup which will be displayed in Figure 6 below.

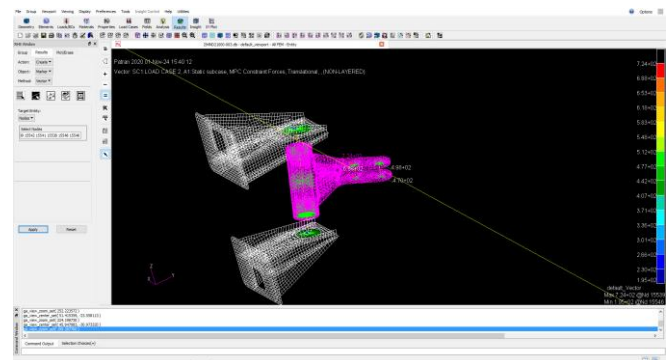


Figure 6: Bearing Strength Plane

The analysis results show that there is no material failure, with a maximum total force on the bearing strength of 724 daN. After calculating the allowable stress permitted for the AL-7050-T7451-AMS 4050 material, a value of 50,986 is obtained. Meanwhile, the applied stress occurring on the bell crank part with a thickness of 6 millimeters and a diameter of

17.46 millimeters is 6,911 daN. If we calculate this using the Margin of Safety equation, the resulting value is:

$$MS = \frac{\sigma_{\text{allowable}}}{\sigma_{\text{applied}}} - 1 \Rightarrow MS = \frac{50,986}{6,911} - 1 = 6.377$$

The above value indicates that the material with a thickness of 6 millimeters meets the safety factor requirements.

3.2.2 Forces at the Bracket Supports

The reaction forces occurring at the MPC supports in the Upper and Lower Brackets show a force of 259 daN on the Upper Bracket and 195 daN on the Lower Bracket. The forces at the bracket supports are shown in Figure 7 below.

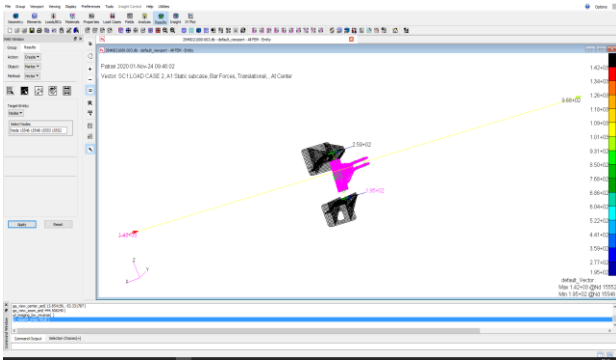


Figure 7: Reaction force at the bracket support

3.2.3 Empirical Calculation

Empirical calculation is a method used to verify force results by comparing simulation calculations with manual output. This is done using analytical formulas, such as the laws of static equilibrium. Static equilibrium applies if the resultant force and moment in a system are equal to zero. The equations 6 are as follows [12]:

$$\Sigma F_x = 0, \quad \Sigma F_y = 0, \quad \Sigma M = 0 \quad (6)$$

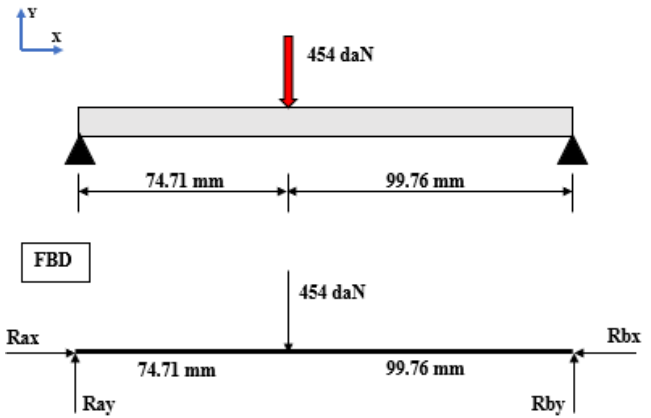
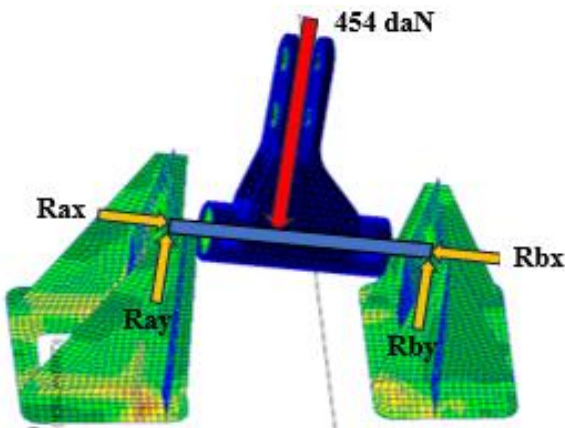


Figure 8: Free Body Diagram of Flight Control Actuator

Empirical calculation results:

$$\Sigma F_x = 0$$

$$\Sigma F_y = 0$$

$$\Rightarrow R_{ay} - 454 (74.71\text{mm}) + R_{by} (174.47\text{mm}) = 0$$

$$R_{by} (174.47\text{mm}) = 33918.34 \text{ daN/mm}^2$$

$$R_{by} = 194.407 \text{ daN/mm}^2$$

$$\Rightarrow R_{by} - 454 (99.76\text{mm}) + R_{ay} (174.47\text{mm}) = 0$$

$$R_{ay} (174.47\text{mm}) = 45291.04 \text{ daN/mm}^2$$

$$R_{ay} = 259.592 \text{ daN/mm}^2$$

3.2.4 Calculating Percentage Error

Calculating the percentage error is a method used to measure the degree of discrepancy or difference between simulation, measurement, or calculation results and a reference value considered correct, such as manual calculations or experimental data. After obtaining both results, a comparison can be made by looking at the percentage difference between the manual calculation and the simulation results [13]. The equation 7 for calculating the percentage error is as follows.

$$\text{Error (\%)} = \left| \frac{\text{Manual Result} - \text{Simulation Result}}{\text{Manual Result}} \right| \times 100\% \quad (7)$$

Based on the stress results appearing in the Multi-Point Constraints (MPC) stress results on the Bracket—which serves as the support for the force transmitted by the Bell crank part—it shows forces of $R_{by} = 195 \text{ daN}$ and $R_{ay} = 259 \text{ daN}$. These values represent the supports for the force applied to the aileron cable. Compared with the hand calculation results,

which are $R_{by} = 194.407$ daN and $R_{ay} = 259.592$ daN, the error percentage can be calculated as follows:

- Error Percentage on Support Ray

$$\text{Error (\%)} = \left| \frac{259.592 - 259}{259.592} \right| \times 100\% = 0.228\%$$

- Error Percentage on Support Rby

$$\text{Error (\%)} = \left| \frac{194.407 - 195}{194.407} \right| \times 100\% = 0.305\%$$

Based on the error calculation results above, it indicates that the stress data results from the MSC Patran and Nastran software are already valid because the resulting tolerance is below 5%.

IV. CONCLUSION

From this simulation, the author can draw several conclusions, including:

- In the analysis using MSC PATRAN and NASTRAN software, sequential methods were used to ensure that all necessary steps in the analysis process could be carried out while considering the problem constraints and avoiding errors during the simulation run.
- From the structural strength simulation using the finite element model performed on the bell crank, the Margin of Safety Index was obtained at 6.377.
- The structural strength of the bell crank, based on the margin of safety index, was positive at 6.377, indicating that the force exerted by the aileron cable of 1422 daN on the bell crank still met the safety factor and was safe for use.

ACKNOWLEDGEMENT

The authors would like to express their sincere gratitude to the Department of Mechanical Engineering, Diponegoro University (UNDIP), for providing the necessary facilities, resources, and continuous support throughout the completion of this research.

REFERENCES

- [1] M. N. Abdullah and I. Maulina, "Sistem Kerja Kelistrikan pada Engine Pesawat Terbang Tipe CRJ-1000," *Elektriase: Jurnal Sains dan Teknologi Elektro*, vol. 14, no. 01, pp. 13–24, 2024. doi: 10.47709/elektriase.v14i01.3739.
- [2] Y. Du, "Advances in flight control systems for modern commercial aircraft," *Journal of Physics: Conference Series* (atau nama

- prosidingterkaitjikaada), vol. 0, pp. 120–126, 2024. doi: 10.54254/2755-2721/103/20241042.
- [3] S. S. Maravajjala, "3D Modelling and Analysis of Bell Crank Mechanism," *International Journal for Research in Applied Science and Engineering Technology*, vol. 8, no. 1, pp. 76–81, Jan. 2020. doi: 10.22214/ijraset.2020.1014.
- [4] A. Harish, "Finite Element Method – What Is It? FEM and FEA Explained," *SimScale*, 2024. Available: <https://www.simscale.com/blog/what-is-finite-element-method/>. [Accessed: Feb. 10, 2026].
- [5] Indonesian Aerospace, "N219 Nurtanio," *PT Dirgantara Indonesia*, 2025. Available: http://www.dirgantara-indonesia.com/aircraft/detail/11_n219+nurtanio.html. [Accessed: Feb. 10, 2026].
- [6] R. Hani, S. Zakiyah, and D. Rusdiana, "Desain Dan Evaluasi Penggunaan Media Pembelajaran Materi Momen Inersia Menggunakan Arduino," *Jurnal Inovasi dan Pembelajaran Fisika*, vol. 10, no. 1, pp. 63–73, 2023. doi: 10.36706/jipf.v10i1.19711.
- [7] B. Purnama and T. Rachman, "Teknik Penanganan Deformasi Pengelasan Elemen Pendukung Konstruksi Bangunan Kapal," *Riset Sains dan Teknologi Kelautan*, pp. 281–286, Nov. 2023. doi: 10.62012/sensistek.v6i2.32548.
- [8] T. Mishra, "Margin of Safety," *Safeopedia*, 2023. Available: <https://www.safeopedia.com/definition/9742/margin-of-safety-engineering>. [Accessed: Feb. 10, 2026].
- [9] A. Toteles and F. Alhaffis, "ANALISIS MATERIAL KONTRUKSI CHASIS MOBIL LISTRIK LAKSAMANA V2 MENGGUNAKAN SOFTWARE AUTODESK INVENTOR," *Machine: Jurnal Teknik Mesin*, vol. 7, no. 1, pp. 30–37, 2021.
- [10] M. O. A. Ferreira et al., "Effect of Nb2O5 coating on the corrosion resistance of the 7050-T7451 aluminium alloy," *Emergent Materials*, vol. 6, no. 4, pp. 1115–1125, 2023. doi: 10.1007/s42247-023-00569-x.
- [11] Hexagon, "MSC Nastran Student Edition," *Hexagon*, 2025. Available: <https://hexagon.com/products/msc-nastran-student-edition>. [Accessed: Feb. 10, 2026].
- [12] H. Gultom, *Statika & Dinamika*, edisi ke-1. Medan: Departemen Teknik Mesin, 2023.
- [13] Saifudin, "Analisis Perbandingan Perhitungan Short Circuit Pada GarduInduk 150 / 20 KV (Studi Kasus Pada GarduInduk Manyar Gresik)," *Jurnal Teknik Elektro*, vol. 10, pp. 507–515, 2021.

Citation of this Article:

Shofwan Bahar, Eflita Yohana, Sri Nugroho, & Margiyanto. (2026). Structural Strength Analysis of Flight Control Actuator Support System Part Bell Crank LH-Wing Using Finite Element Method on NXXX Aircraft. *International Research Journal of Innovations in Engineering and Technology - IRJIET*, 10(5), 530-536. Article DOI <https://doi.org/10.47001/IRJIET/2026.105073>
